Charge transport in mixed CdSe and CdTe colloidal nanocrystal films

Scott Geyer,[1] Venda J. Porter,[1] Jonathan E. Halpert,[1] Tamar S. Mentzel,[2] Marc A. Kastner,[2] and Moungi G. Bawendi[1,*]

[1]*Department of Chemistry, Massachusetts Institute of Technology,*
77 Massachusetts Avenue, Cambridge, Massachusetts 02139, USA

[2]*Department of Physics, Massachusetts Institute of Technology, 77 Massachusetts Avenue, Cambridge, Massachusetts 02139, USA*

We report the influence of trap states on charge transport through films of mixed CdTe and CdSe nanocrystals (NCs) between lateral electrodes, through layered films of CdTe and CdSe NCs in a layered geometry, and through films of CdTe/CdSe nanobarbells in a layered geometry. We find that an electron trapping state on the surface of the CdTe NCs dominates the conduction in all devices studied. X-ray photoelectron spectroscopy and thermal activation studies implicate unpassivated or oxidized Te as the electron-trapping site.

I. INTRODUCTION

There is considerable interest in colloidal semiconductor nanocrystals (NCs) as active components for the next generation of solar cells and other optoelectronic devices. Potential advantages of colloidal NCs are that they can be deposited on any surface and that the band gap of a NC can be tuned by changing the size of the particle.[1,2] However, with the advantages of NCs come challenges because the organic ligands, which allow for the solution processing of the NCs, inhibit exciton separation and decrease charge-carrier mobility in close-packed NC films.[3–8] The large surface-to-volume ratio of the NC also results in more unpassivated surface atoms, which may serve as trap states, than would be present in a bulk semiconductor film. Such traps increase the probability for recombination in the bulk of the film, rather than extraction at the electrodes.[9]

The band gap of CdTe NCs can be tuned from 1.5 to 2.1 eV,[2] covering most of the range of the peak emission power of the solar spectrum.[10] CdSe/CdTe heterojunction solar cells displaying 2.9% efficiency processed from sintered NCs have been reported;[11] however, this value is still low when compared to the 16.5% efficiency which has been reported for CdTe/CdS thin-film solar cells[12] and 13.6% for CdTe thin-film solar cells on flexible substrates.[13] In addition, this efficiency is not achieved until the NCs are sintered together, burning away most of the organic ligands in the process, losing the quantum-mechanical confinement and effectively creating a nanocrystalline thin film.[11] While spinning NCs from solution and then sintering may constitute an alternative route to bulk semiconductor thin films, many of the potential advantages offered by quantum-confined NCs are lost in the process. In order to increase the efficiency of NC photovoltaic and other optoelectronic devices, the physics of charge transport through NC films needs to be well characterized so that methods can be developed to improve the extraction of charge from NC films while keeping intact quantum-confinement effects.

In this paper, the photoconductivity of films composed of both CdSe and CdTe NCs, and CdSe/CdTe nanobarbells (NBs) is investigated. CdSe adjacent to CdTe forms a type-II heterojunction, in which the band offset of the two semiconductors separates excitons at the interface with electrons in CdSe and holes in CdTe. Infrared emission from type-II core/shell CdTe/CdSe NCs demonstrates that the type-II effect is indeed present in NC materials.[14] By mixing CdTe and CdSe NCs together, numerous type-II interfaces are created throughout the film and charge transport can, in principle, proceed by electron carriers through a percolating CdSe network and hole carriers through a CdTe network, reducing carrier recombination in the film. However, we find that charge trapping at NC surface states overwhelms the effect of the type-II interfaces. Specifically, an electron acceptor state on the surface of CdTe NCs is found to trap electrons in our thin-film NC devices. We present a detailed characterization of the electrical consequences of this surface state in mixed CdTe/CdSe NC and CdTe/CdSe nanobarbell photoconductive and photovoltaic devices.

II. EXPERIMENTAL

A. Synthesis

CdTe and CdSe NCs were synthesized using standard methods for II-VI NC synthesis[15,16] and CdSe/CdTe rod/dot NBs (CdSe/CdTe NBs) were synthesized using a previously published procedure.[17,18] The CdTe NCs were 6 nm in diameter and the CdSe NCs were 4.9 nm in diameter. The nanobarbells consisted of CdSe nanorods (NRs) that were ∼15 nm in length and ∼5 nm in diameter with CdTe NCs at each end of each rod that were 5.5–6 nm in diameter.

B. NC film and device preparation

Two measurement devices were used in this study. (1) The lateral device [Fig. 1(a)] was a silicon inverted field-effect transistor (FET). The FETs were fabricated by lithographically patterning gold bar electrodes $200 \times 800 \times 0.1$ μm^3 on 330-nm-thick silicon oxide. The electrodes were separated by 1 or 2 μm. (2) The layered device [Fig. 1(b)] consisted of a transparent bottom electrode; 20 nm poly(3,4-ethylenedioxythiophene) poly(styrenesulfonate) (PEDOT-:PSS) spin-coated onto indium-tin oxide (ITO). The photoactive layer consisted of multiple, discrete, ∼25-nm-thick layers of CdTe NCs, CdSe NCs, or CdSe/CdTe NBs spun from chloroform and treated with a solution of butylamine in acetonitrile to decrease interparticle spacing. The top electrode was a eutectic gallium-indium solder (EGaIn).[19]
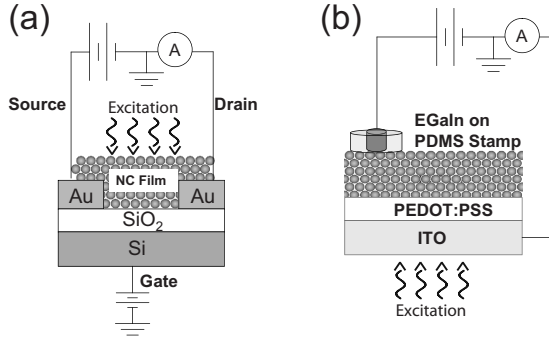
FIG. 1. Schematic of the devices used in the experiments. (a) Lateral device structure consisting of gold electrodes $200 \times 800 \times 0.1$ μm patterned on 330 nm silicon oxide on a silicon backgate or quartz (not shown). The electrodes are spaced by 1 or 2 μm. The NC film, typically 100–200 nm thick, was drop cast or spun onto the device and covers the entire surface of the device. (b) Layered device structure used in the photovoltaic study. 20-nm-thick PE-DOT:PSS was deposited onto ITO covered glass. NC layers, each ~25 nm thick, are spun on top of the PEDOT:PSS. The top contact was a EGaIn which was set in a thin PDMS donut (3.5 mm outer diameter, 1.5 mm inner diameter). The EGaIn settles in the area defined by the PDMS donut and forms a conformal contact with the NC film. The EGaIn was contacted with a Pt wire and the ITO with a metal pin. Photoexcitation occurs through the ITO face of the device.

The film treatment employed in this paper is postdeposition cap exchange with butylamine.[5] For the butylamine cap exchange, the NC film was soaked in a 0.1 M solution of butylamine in acetonitrile for 2 min. The film was then rinsed in acetonitrile and baked in a nitrogen environment for 1 h at 70 C to remove excess solvent.

C. Electrical measurements

All conductivity measurements on lateral devices were performed in a Janis VPF-100 cryostat under vacuum. Samples were loaded into the cryostat in the glovebox and never exposed to air. An Ar$^+$ laser at 514 nm was used to photoexcite the samples. It has been shown previously that photocurrent is not a result of photoinjection from the electrodes.[6] For the layered devices, the current was measured in air with the incident light going through the ITO face first. The EGaIn electrode wets the NC film surface through a 1.5 mm radius hole cut in a thin piece of polydimethylsiloxane (PDMS). Both the PDMS and EGaIn conformably contact the surface of the NCs. For photocurrent action (PCA) spectra measurements in which the photocurrent was measured as a function of the wavelength of the excitation light, the samples are photoexcited with a 150 W ozone free xenon arc lamp through a monochromator. The photovoltaic and photoconductive external quantum efficiencies are determined using a silicon photodiode (Thorlabs DET210) as a reference.

D. Optical measurements

The absorbance spectrum of the NC films on glass slides was measured with a Cary 5000 UV-visible-near infrared
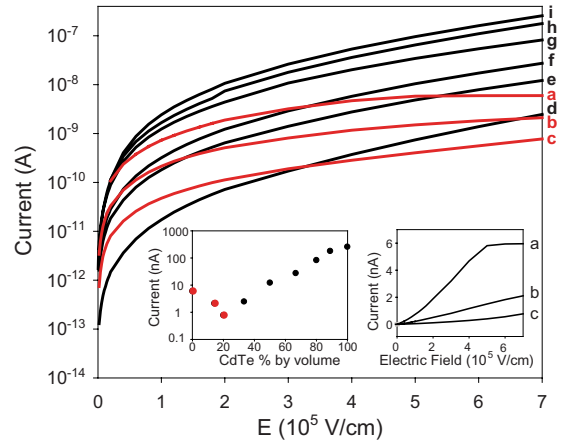

FIG. 2. (Color online) Photocurrent versus electric field with 32 mW/cm^2 514 nm excitation for mixed films composed of CdTe and CdSe NCs. Each line represents the photocurrent measured in a film containing a different ratio by volume of CdTe to CdSe: (a) 100% CdSe, (b) 14% CdTe, (c) 20% CdTe, (d) 33% CdTe, (e) 50% CdTe, (f) 66% CdTe, (g) 80% CdTe, (h) 88% CdTe, and (i) 100% CdTe. The left inset displays the magnitude of the photocurrent at 7×10^5 V/cm as a function of volume percent of CdTe. The red lines and circles designate films in which the field dependence of the photocurrent resembles that of an all-CdSe NC film while the black lines designate those films in which it resembles the field dependence of the photocurrent through the all CdTe NC film. The right inset shows the photocurrent curves (a)–(c) plotted on a linear scale versus electric field, demonstrating the saturation of the 100% CdSe NC film and the loss of saturation with the addition of CdTe NCs.

spectrometer. Fluorescence measurements were performed using a Horiba Jobin-Yvon Fluoromax-3 spectrometer. The fluorescence quantum yield (QY) of CdTe NCs was calculated using oxazine 720 as the reference dye. The QY of this dye at room temperature is 60% in ethanol and 63% in methanol.[20]

III. RESULTS

A. Conductivity of mixed films of CdTe and CdSe NCs and films of CdSe/CdTe NBs

1. CdSe and CdTe mixed NC films

Figure 2 shows the field dependence of the photogenerated current for films composed of varying ratios of CdSe NCs to CdTe NCs in the lateral device geometry [Fig. 1(a)]. Films containing only CdSe NCs (trace a) show photocurrent saturation with electric field, indicating efficient extraction of both carriers and blocking contacts, as discussed below, while films containing over 20% CdTe NCs by volume (traces d–i) exhibit photoconductive gain and do not saturate with electric field in the field range studied. Films with a small percentage of CdTe NCs (traces b and c) show decreased photocurrent compared to the pure CdSe NC film and no longer exhibit saturation under the fields used in this study. The magnitude of the photocurrent reaches a minimum at 20% CdTe NCs by volume, as shown in the inset of Fig. 2.
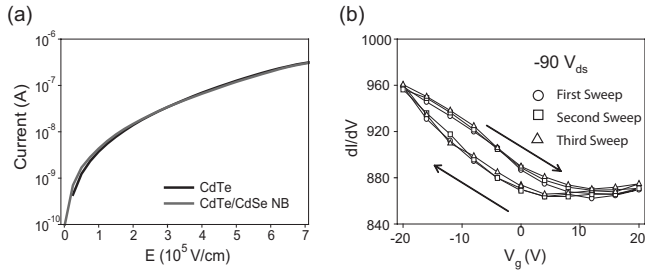
FIG. 3. (a) Photocurrent versus electric field with 32 mW/cm^2 514 nm excitation for a CdTe NC film (black line) and a CdSe/CdTe NB film (gray line). The magnitude of the photocurrent has not been scaled for either of the films but they are matched to have a similar absorbance value at 514 nm. (b) Room-temperature differential conductance dI/dV plotted as a function of gate voltage for a CdSe/CdTe NB film held at -90 V_{ds}. V_g is applied for 5 s and followed by a recovery of 5 s at 0 V_g before V_g is stepped to the next value (Ref. 18).

2. CdSe/CdTe NB films

Figure 3(a) shows the field dependence of the photocurrent of a CdSe/CdTe NB film compared to a CdTe NC film. The field dependence of the photoconductivity for films of CdSe/CdTe NBs is nearly identical to that of films composed entirely of CdTe NCs. In Fig. 3(b) we show differential conductance measurements of the NB films as a function of voltage on the Si substrate, used as a gate [see Fig. 1(a)]. The dark conductance increases with negative gate voltage indicating that holes are the majority carrier. Temperature-dependence measurements of the dark current in NB films yields an activation energy of 0.33 eV for the dark current, nearly identical to that of CdTe NC films.[15,18]

B. Oxidation and modification of CdTe NC surface

Figure 4 shows the dark conductivity and photoconductivity of a CdTe NC film as a function of field and air expo-
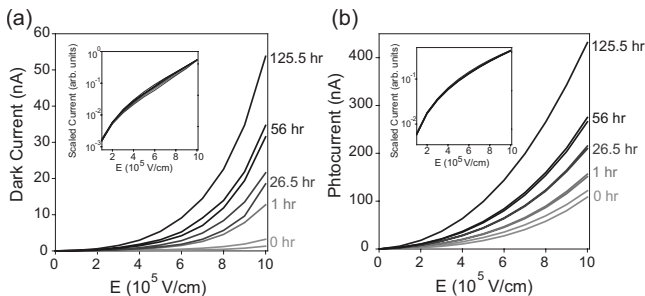

FIG. 4. Room-temperature (a) dark and (b) photocurrent current-field curves as a function of exposure to air. The electric field is swept from 0 to 10×10^5 V/cm for each curve. Two curves are taken at each air exposure time to demonstrate that it is the air exposure and not sweeping of the electric field, which results in the enhancement of the current. The insets of graphs (a) and (b) are the same data scaled in current and plotted on a log plot to highlight the electric field dependence of the current. The current is measured in a cryostat under vacuum and then the sample is opened to air for the designated period of time.
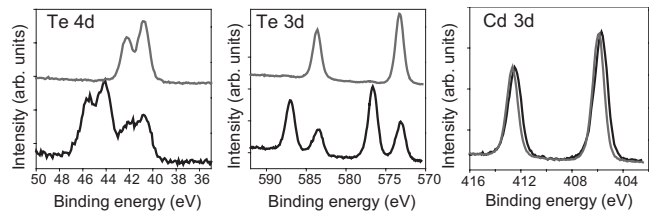

FIG. 5. XPS spectra for a CdTe NC film before (gray line) and after (black line) exposure to air for 3 weeks. Characteristic Te 4d, Te 3d, and Cd 3d peaks are shown before (gray) and after (black) oxidation of the CdTe NC film. The unoxidized Te 4d doublet located at 40.73 and 42.2 eV is assigned to Te-Cd in accordance with bulk CdTe values (Ref. 21). In the Te 4d and Te 3d spectra of the oxidized film additional peaks appear shifted $\sim$3.5 eV to higher binding energy. These are attributed to TeO$_2$ and CdTeO$_3$ surface states. The Cd 3d peak shows only a slight shift to higher energies, possibly due to Cd-O formation or oxidation of the ligands which are bonded to the Cd.

sure. An increase in both the dark current and photocurrent is observed with increasing exposure time to air under ambient conditions while the insets in Figs. 4(a) and 4(b) show that the overall shape of the field dependence remains largely unchanged.

In Fig. 5, x-ray photoelectron spectroscopy (XPS) data for CdTe nanocrystal films processed under inert conditions are compared to identically prepared films exposed to air for 3 weeks. The 3.5 eV shift of the Te 4d spectrum upon oxidation is consistent with observations in Ref. 21 where a $\sim$3.7 eV shift is proposed to correspond to Te in the +4 oxidation state and TeO$_2$ and CdTeO$_3$ are proposed as the surface states.[21]

Exposure of CdTe NCs in solution or in a thin film to oxygen results in rapid quenching of the photoluminescence. It has been shown that CdTe NCs with a Cd-rich surface have a higher photoluminescent QY in air than those with a Te-rich surface.[22] After three precipitations and redispersion in hexane, the QY of the CdTe NC solution is $\sim$0.1%. However, after addition of cadmium oleate the QY increases to as much as 50% and remains fluorescent for weeks when stored in air.[18]

Layered CdTe and CdSe nanocrystal thin-films photovoltaics

Three-layered device structures with CdTe and CdSe NCs and CdTe/CdSe NBs have been constructed. In each device the bottom contact is a transparent electrode, ITO coated with 20 nm of PEDOT:PSS; each nanocrystal layer is 25 nm thick, and the top electrode is a EGaIn. The ITO is connected to ground and voltage is applied to the EGaIn contact. In contrast to the previous experiments, all measurements here are conducted in air.

Device #1 consists of ITO, PEDOT:PSS, a CdTe NC layer (band-edge absorption at 660 nm), a CdSe NC layer (band-edge absorption at 600 nm), and EGaIn, in that order. The band diagram, depicted in Fig. 6(a), shows the positions of the work functions and conduction and valence bands for the metals and semiconductors, respectively. These values represent the individual material properties prior to establishment
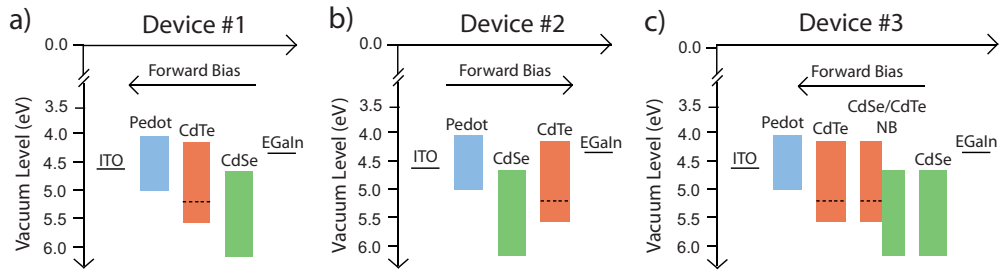
FIG. 6. (Color online) Energy-level diagrams for (a) device #1, (b) device #2, and (c) device #3. Energies are given relative to vacuum level and represent the values for each component prior to establishment of a uniform Fermi level across the device (band bending). For the ITO and EGaIn electrodes, the lines indicate the work functions of the metals. For the semiconductor materials, the bottom of the rectangle indicates the position of the valence band and the top of the rectangle indicates the position of the conduction band. The dotted line indicates the position of the proposed electron trapping state on the CdTe NC surface. All devices exhibit diode behavior and the arrows indicate the direction of forward bias in each device (see discussion).

of a uniform Fermi level across the device. The PCA spectra and absorbance spectrum for this device are shown in Fig. 7(b). Comparison with the absorption spectra of CdSe NCs and CdTe NCs [Fig. 7(a)] shows that at zero bias the photocurrent comes primarily from the CdSe NC layer and there is little contribution from the CdTe NC layer. The limited contribution of CdTe NCs to the photocurrent is not a consequence of optical screening by the CdSe layer since the CdTe layer absorbs to the red of the CdSe layer, as indicated by their respective solution phase absorption spectra in Fig. 7(a). When 0.6 V is applied to the EGaIn, the device is in

reverse bias and the PCA spectrum still appears to only come from CdSe NCs. However, when −0.6 V forward bias is applied the majority of the photocurrent in the PCA spectrum comes from excitons absorbed in the CdTe layer.

Device #2 is a variation in device #1 with the order of the NC layers reversed; it consists of ITO, PEDOT:PSS, a CdSe NC layer, a CdTe NC layer, and EGaIn in that order [Fig. 6(b)]. At zero bias the photocurrent flows in the opposite direction of device #1 and the external quantum efficiency (EQE) is an order of magnitude lower, as shown in Fig. 7(c). Like device #1, the PCA spectrum indicates that only exci-
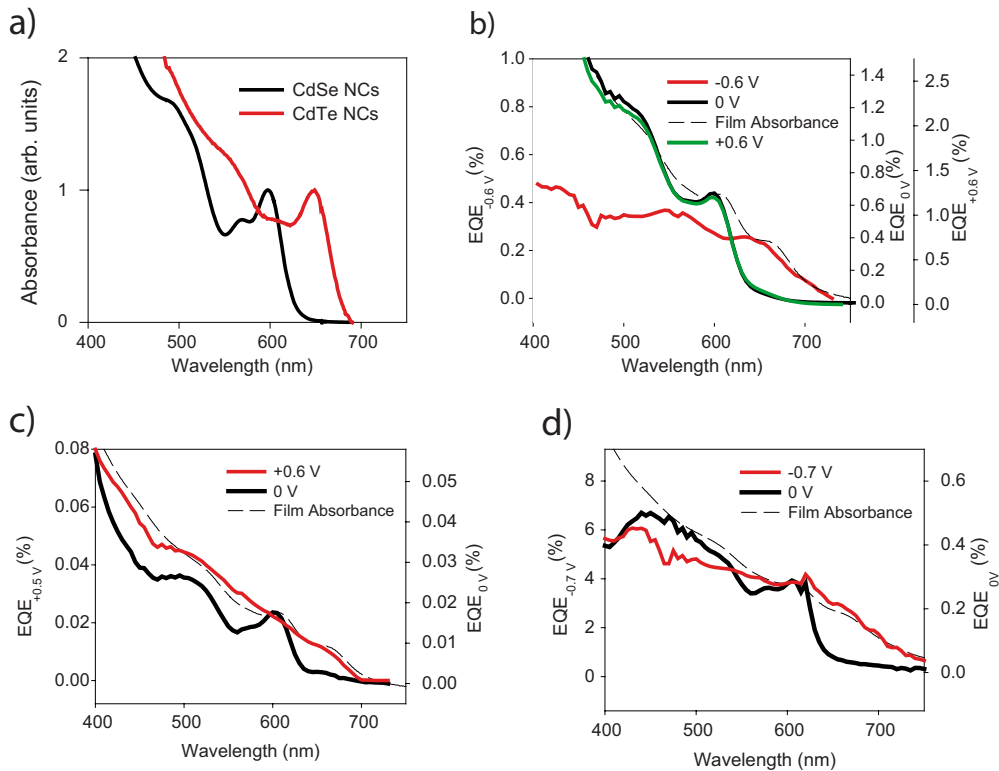

FIG. 7. (Color online) (a) The absorption spectra of CdSe and CdTe NCs in solution. (b) The PCA spectra for device structure #1 is displayed at 0 V (black line), +0.6 V (green line, same as 0 V), and −0.6 V (red line). The absorbance of device #1 is given by the dotted line. (c) The PCA spectra for device #2 is displayed at 0 V (black line) and +0.6 V (gray line). The absorbance of device #2 is given by the dotted line. (d) The PCA spectra for device #3 is displayed at 0 V (black line) and +0.6 V (red line). The absorbance of device #3 is given by the dotted line.
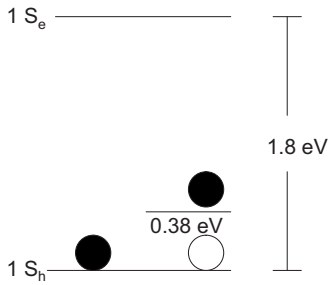
FIG. 8. Energy-level diagram for a CdTe NC with an acceptor state 0.38 eV from the valence band denoted by $1S_h$. We ignore any intrinsic width of the valence and conduction bands. At room temperature this state can be populated with electrons (black circles) thermally excited from the valence band, leaving holes behind (white circles). As the temperature decreases, the number of electrons in the acceptor state (and thus the hole density) decreases.

tons generated in the CdSe NC layer contribute to the photocurrent at zero bias while under forward bias, which corresponds to positive voltage applied to the EGaIn for device #2, a contribution from the CdTe NC layer is clearly visible. CdSe/CdTe NBs are included in device #3 which consists of ITO, a CdTe NC layer, a CdSe/CdTe NB layer, a CdSe NC layer, and EGaIn in that order [Fig. 6(c)]. Like device #1, device #3 is forward biased when negative voltage is applied to the EGaIn. At zero bias the photocurrent comes mainly from the CdSe NC layer while under forward bias the NB and CdTe NC layers contribute to the photocurrent [Fig. 7(d)].

IV. DISCUSSION

A. Conductivity in CdTe NC films—A review and further insights on charge transport mechanisms in CdTe NC films

In previous investigations of the dark and photogenerated current in butylamine capped CdTe NC films between gold electrodes, differential conductance measurements have revealed that holes are the majority carrier of the dark current.[15] The room-temperature dark current is found to be steady state, an indication that the gold electrodes can inject holes into the CdTe NC film, unlike the case of CdSe NC films.[3] This is consistent with the small (0.4 eV) difference between the work function of gold (5.1 eV) and the valence band of CdTe (5.5 eV). Holes are found to be generated by the thermal excitation of valence-band electrons with a thermal activation energy of 0.38 ± 0.02 eV, which we interpret as the energy difference between the acceptor state and the valence band (Fig. 8) as found in other NC films.[28] We now present an analysis of this state including its physical origin and its effect on the conduction mechanism of films incorporating CdTe NCs.

In bulk CdTe, a cadmium vacancy in the lattice results in an electron acceptor state located 0.3 eV from the valence band.[23] The surface of a CdTe NC contains tellurium atoms, many of which may be unpassivated. It is possible that unpassivated tellurium atoms, i.e., cadmium vacancies on the surface or additional cadmium vacancies in the lattice are responsible for the electron accepting state in NCs. There is

also evidence that an oxidized form of Te may be the acceptor state because the dark current increases with exposure to air as demonstrated in Fig. 4(a). The XPS results (Fig. 5) confirm that oxygen exposure alters the surface of the CdTe NC with clear new peaks in the Te $3d$ and Te $4d$ XPS spectra appearing after oxidation. These are assigned to Te in the 4+ oxidation state, consistent with TeO_2 or $CdTeO_3$ being the surface state.[21]

The CdTe NCs are kept under argon during synthesis, transferred to a nitrogen glove box for processing, and measured under vacuum in a cryostat loaded in the glovebox. However, none of these processes are fully oxygen free, and it is possible that some percentage of the surface tellurium atoms have been oxidized. In our proposed mechanism, prolonged air exposure creates more oxidized tellurium sites which can accept electrons from the valence band, and thus creates a larger density of holes. It should be noted that, as the inset of [Fig. 4(a)] demonstrates, only the magnitude and not the electric field dependence of the dark current varies significantly with oxygen exposure. In other words, oxidation of the CdTe NCs results in a higher hole carrier density but does not change the conduction mechanism.

The photocurrent in CdTe NC films is secondary with a photoconductive gain (number of times a charge-carrier cycles through the device) greater than one. This mechanism has been explored in detail in a previous publication.[15] In general, secondary photocurrents with gains greater than one occur when the electrodes can inject electrons and/or holes, and when the mobility of one of the charge carriers is higher than the other.[23] The carrier with the higher mobility cycles through the circuit until it recombines with the slower carrier or until the slower carrier reaches an electrode for extraction. Since the photocurrent is found to have a gain greater than one and, as discussed previously, only the hole is replenished from the gold electrodes, the hole must have a higher mobility than the electron in CdTe NC films. This is surprising because in bulk CdTe the effective mass of the hole is $0.63m_o$, larger than the $0.11m_o$ effective mass of the electron.[24] This result can be explained if the electron accepting state at 0.38 eV accepts electrons from the conduction band as well as the valence band. When electrons are thermally excited from the valence band the state behaves as a doping state, increasing the hole density. However, when the state accepts electrons from the conduction band the electron is deeply trapped. This state is 1.4 eV from the conduction band so it is unlikely that electrons can be thermally excited out of the state, and therefore the average electron mobility is greatly reduced. Electrons remain in this state until they recombine with holes so the state could also be termed a recombination center with a minor affinity for holes.

This model is consistent with the effects of oxygen exposure on the dark and photogenerated current in CdTe films presented in Fig. 4. A simultaneous increase in both the dark and photogenerated current may appear surprising, since an increase in the dark hole density should lead to a shorter lifetime of the electron in the conduction band, which, in general, results in a reduction in the photocurrent. However, if the acceptor state acts as a long-lived recombination center for electrons, the addition of new acceptor states upon oxidation may actually extend the lifetime of the photogener-

ated electron, resulting in an increase in the gain and increased photocurrent.

In addition to altering the conductivity of CdTe NC films, air exposure strongly quenches the fluorescence of CdTe NCs, and this fluorescence quenching is correlated with the formation of oxidized tellurium atoms (Te-O) on the surface of the nanocrystal.[21] The fluorescence quenching may be a result of fast exciton dissociation due to rapid capture of the electron by the oxidized tellurium state. The post synthetic addition of cadmium oleate to CdTe NCs to form a cadmium-rich surface is shown to increase the quantum yield of the CdTe NCs dramatically from 0.1% to 50% and reduce the rate of fluorescence quenching upon exposure to oxygen. If Cd atoms cover the surface, this could slow down the rate of formation of a Te-O complex on the nanocrystal surface, consistent with the increase in quantum yield and stability.

In summary, an electron accepting state on the surface of CdTe NCs is responsible for the *p*-type dark current because it accepts thermally excited electrons from the valence band, leaving holes behind. This same state may also be responsible for exciton separation by accepting electrons from the conduction band. These electrons remain trapped in this state until they recombine with a hole, offering an explanation for why the effective hole mobility is larger than the electron mobility in CdTe NC films.

B. Mixed films of CdTe and CdSe NCs and CdSe/CdTe NB films between lateral electrodes—Photoconductive mode

Films composed of mixed CdTe and CdSe NCs should theoretically aid exciton separation compared to pure films of CdTe or CdSe NCs because the two bulk materials form a type-II junction when they are juxtaposed. Ideally, an exciton near the interface would be separated by the junction between CdTe and CdSe NCs, with the electron residing in the CdSe NCs and hole in the CdTe NCs after separation. The type-II offset should reduce the voltage necessary for exciton separation and the resulting spatial separation of the charges should also increase the lifetime of the free carriers.

Saturation of the photocurrent with voltage, seen only in films of CdSe NCs (Fig. 2) occurs when the transit time of the less mobile charge carrier is shorter than the recombination lifetime and the electrodes form blocking contacts.[23] If the mixed films of CdSe NCs and CdTe NCs were to exhibit saturation, it would indicate that the electrons were efficiently extracted from the mixed films. Because of the type-II band offset, we would expect the CdTe NC/CdSe NC film to show photocurrent saturation at a lower applied field than for pure CdSe NC films, since the voltage required for exciton separation should be lowered by the type-II interface and the recombination lifetime should be increased by the spatial separation between the electron and hole in the two types of NCs. The second requirement for saturation, the presence of blocking contacts, is not satisfied for films of CdTe NCs. The observed photoconductive gain in CdTe NC films between gold electrodes indicates that gold does not form a hole-blocking contact with CdTe NCs.[15] However, since the conduction band of CdTe NCs is ~1.4 eV above

the vacuum level of gold, gold is expected to form a blocking contact for electron injection with CdTe NCs. In this case, once the electron lifetime is as great as the electron transit time saturation of the photocurrent should still be observed.

For the case of CdSe/CdTe NBs, the CdTe NC is directly connected to the CdSe NCs, which should increase the probability of type-II exciton separation since there is no longer an organic tunneling barrier between the CdSe and CdTe NCs, as is the case for the mixed films. In addition, the ratio of CdTe to CdSe is uniform throughout the film, eliminating potential difficulties stemming from segregation of CdTe and CdSe NCs.

The benefits of a type-II heterojunction as discussed above are clearly not observed for films of mixed CdSe and CdTe NCs (Fig. 2). When the film is composed entirely of CdSe NCs, both the electron and hole can be extracted from the film; however, as the ratio of CdTe to CdSe NCs increases more electrons become trapped and the photocurrent does not saturate. When the film is about 33% CdTe NCs, the photocurrent vs electric field curve closely resembles that of the 100% CdTe NC film indicating similar conduction mechanisms in both systems. From 33% CdTe NCs, increasing the percentage of CdTe NCs in the film increases the magnitude of the photocurrent as there are fewer CdSe NCs to slow the conduction of holes. CdSe NCs could, in principle, conduct holes, but the valence band is located ~1.2 eV below that of CdTe and so extra energy must be supplied to conduct through the CdSe NCs. The minimum in conduction at 20% CdTe concentration is most likely a reflection of a percolation threshold in which CdTe NCs are spaced too far apart for hole conduction between CdTe NCs, but present in high enough concentration to lower electron mobility. Theoretical calculations of the percolation threshold for randomly packed hard spheres and closest packed hard spheres (NC films after chemical treatment or annealing likely exist somewhere between the two regimes) give a critical volume fraction for percolation of 18% and 15%, respectively, close to the minimum observed in the inset of Fig. 2.[25] In CdSe/CdTe NBs films, where the CdTe concentration is well above the percolation threshold, a nearly identical field dependence of the photoconductivity to films of pure CdTe NCs is observed (Fig. 3), indicating that for this material the CdTe trap state may be dominating the electron conduction.

Photoexcited electrons may enter the CdTe trap state directly from the CdSe conduction band since the energy of the CdTe electron trap state is lower than the energy of the conduction band of CdSe. Given the large energy offset between the CdTe and CdSe conduction bands, it is unlikely that a free electron first hops into the CdTe conduction band before being trapped. However, exciton diffusion may also lead to decreased electron mobility in these films. In this model, the exciton diffuses from CdSe to CdTe NCs by Förster resonance energy transfer (FRET). Efficient FRET transfer has been demonstrated in films of CdSe NCs (Ref. 26) and films of CdTe NCs.[27] Since the band gap of CdTe is smaller than CdSe, there is no spectral overlap for the reverse process so the exciton becomes trapped in CdTe. The electron acceptor state may then directly trap the conduction-band electron, breaking apart the exciton.

In conclusion, in both mixed films of CdTe and CdSe NCs and CdSe/CdTe NBs the electron trapping on the CdTe NC surface dominates charge transport through the films. Even if excitons are ionized at the type-II interface, electron transport does not appear to be segregated to the CdSe NCs and NRs and electrons still end up deeply trapped at the surface of the CdTe nanoparticle.

C. Layered CdTe and CdSe nanocrystal thin-films photovoltaics

While photoconductive devices with gains greater than unity can be useful for photodetectors, they do not increase the efficiency of a photovoltaic device. Unlike a photoconductive device, a photovoltaic device requires that both charges be extracted at the electrodes. The low efficiencies of many NC/polymer hybrid solar cells is attributed in part to trapping states in the NC/polymer film which cause charge carriers to recombine before they can be extracted at the electrodes.[9] The CdTe NC films and CdSe/CdTe NB films between lateral gold electrodes described above behave as secondary photoconductors with the hole amplifying the current as it cycles through the circuit a number of times before recombining with a trapped electron. If these materials are to work in a photovoltaic device, the electron must be able to reach an electrode for extraction.

The first device studied (Fig. 6) is a type-II planar heterojunction between CdSe NCs and CdTe NCs. The photoaction spectrum of the device reveals a minimal contribution to the photocurrent from the CdTe layer compared to the contribution from the CdSe layer. If excitons diffused efficiently to the interface from both layers and separated across the type-II junction, then excitons created in both layers should contribute to the photoaction spectrum relative to the strength of their absorption. If the main source of free carriers is separation at the interface, then minimal contribution to the photocurrent from the CdTe layer suggests that the exciton diffusion length in the CdTe nanocrystals is much shorter than the diffusion length in CdSe. The dramatic quenching of photoluminescence of CdTe when exposed to oxygen indicates that the exciton lifetime is much shorter in air-exposed CdTe NCs than air-exposed CdSe NCs, which may result in a shorter diffusion length. The electrons trapped in the CdTe NCs are immobile and unable to reach the CdSe NC film to conduct, preventing photons absorbed in the CdTe layer from generating a current in the device.

Under forward bias, the contribution of CdTe NCs to the photoaction spectrum becomes apparent. In forward bias, holes can be injected from the ITO into the PEDOT:PSS and subsequently into the CdTe. This means that holes that recombine at the interface with electrons in CdSe can be replenished from the contacts, causing current to flow. Alternately, the current may arise from exciton separation at the interface with PEDOT:PSS with the electron recombining in the *p*-type polymer. Either way, the effect of the photons absorbed by CdTe NCs is to increase the hole density in the CdTe NC film at equilibrium.

Device 2 is identical to device 1 with the exception that the order of the CdTe and CdSe NC layers are reversed. In this case, the built in field created by the work function offset of the metal electrodes opposes the built in field generated by the CdTe/CdSe heterojunction. The direction of photogenerated current flow at zero bias is reversed compared to device 1, indicating that the electrochemical potential difference between the CdSe NC layer and the CdTe NC layer is larger than that between the electrode materials. The EQE of device 2 is an order of magnitude smaller than that of device 1 as expected given the nonideal geometry of the device. As in device 1, the CdTe absorption only contributes strongly to the PCA spectrum under forward bias, indicating that the behavior observed in device 1 is not unique to the CdTe NC and PEDOT:PSS interface.

Device 3 is identical to device 1 with the addition of a NB film between the CdTe and CdSe NC layers, forming a bulk heterojunction layer. Although the previous devices indicate that at zero bias the CdTe NC film does not contribute to the photocurrent, ideally the CdSe/CdTe NB film would exhibit better transport properties. However, as observed in the mixed NC films, the NB layer appears to act similarly to the CdTe layer since it does not contribute to the zero-bias PCA spectrum.

To summarize, the three photovoltaic devices with different combinations of CdTe NCs, CdSe NCs, and NBs all exhibit contributions to the photocurrent only from the CdSe NC layer when measured at zero applied bias. The CdTe NC and CdSe/CdTe NB layers contribute to the photocurrent only when the device is run in forward bias. These results are consistent with the trapping of electrons by the CdTe surface state described in the previous section.

V. CONCLUSIONS

We find that unpassivated and/or oxidized atoms on the surface of CdTe NCs serve to deeply trap electrons and enhance the exciton ionization rate. Experiments with mixed films of CdTe and CdSe NCs and CdSe/CdTe NBs in a planar device geometry all display conductivity properties that can be linked to the trapping of electrons on the surface of the CdTe NCs. These trap states hinder CdTe NCs from contributing to the photocurrent in a NC-based photovoltaic device at zero or reverse bias. These results demonstrate the importance of surface states in influencing the conduction in both homogenous and heterogeneous NC-based devices.

[1] C. B. Murray, D. J. Norris, and M. G. Bawendi, J. Am. Chem. Soc. **115**, 8706 (1993).

[2] Z. A. Peng and X. Peng, J. Am. Chem. Soc. **123**, 183 (2001).

[3] N. Y. Morgan, C. A. Leatherdale, M. Drndić, M. V. Jarosz, M. A. Kastner, and M. Bawendi, Phys. Rev. B **66**, 075339 (2002).

[4] M. Drndić, M. V. Jarosz, N. Y. Morgan, M. A. Kastner, and M. G. Bawendi, J. Appl. Phys. **92**, 7498 (2002).

[5] M. V. Jarosz, V. J. Porter, B. R. Fisher, M. A. Kastner, and M. G. Bawendi, Phys. Rev. B **70**, 195327 (2004).

[6] C. A. Leatherdale, C. R. Kagan, N. Y. Morgan, S. A. Empedocles, M. A. Kastner, and M. G. Bawendi, Phys. Rev. B **62**, 2669 (2000).

[7] C. B. Murray, C. R. Kagan, and M. G. Bawendi, Annu. Rev. Mater. Sci. **30**, 545 (2000).

[8] C. Kagan, Ph.D. thesis, Massachusetts Institute of Technology, 1996.

[9] W. U. Huynh, J. J. Dittmer, and A. P. Alivisatos, Science **295**, 2425 (2002).

[10] J. Orton, *The Story of Semiconductors* (Oxford University Press, New York, 2004).

[11] I. Gur, N. A. Fromer, M. L. Geier, and A. P. Alivisatos, Science **310**, 462 (2005).

[12] A. Morales-Acevedo, Sol. Energy Mater. Sol. Cells **90**, 2213 (2006).

[13] A. Romeo, G. Khrypunov, F. Kurdesau, M. Arnold, D. L. Bätzner, H. Zogg, and A. N. Tiwari, Sol. Energy Mater. Sol. Cells **90**, 3407 (2006).

[14] S. Kim, Y. T. Lim, E. G. Soltesz, A. M. De Grand, J. Lee, A. Nakayama, J. A. Parker, T. Mihaljevic, R. G. Laurence, D. M. Dor, L. H. Cohn, M. G. Bawendi, and J. V. Frangioni, Nat. Biotechnol. **22**, 93 (2004).

[15] V. J. Porter, T. Mentzel, S. Charpentier, M. A. Kastner, and M. G. Bawendi, Phys. Rev. B **73**, 155303 (2006).

[16] P. T. Snee, Y. Chan, D. G. Nocera, and M. G. Bawendi, Adv. Mater. **17**, 1131 (2005).

[17] J. E. Halpert, V. J. Porter, J. P. Zimmer, and M. G. Bawendi, J. Am. Chem. Soc. **128**, 12590 (2006).

[18] See supplementary material at http://link.aps.org/supplemental/10.1103/PhysRevB.82.155201 for more detailed synthesis information, a detailed description of the differential conductance measurement, the details on the experiment apparatus and raw data, and a discussion of the cadmium oleate treatment.

[19] E. A. Weiss, R. C. Chiechi, S. M. Geyer, V. J. Porter, D. C. Bell, M. G. Bawendi, and G. M. Whitesides, J. Am. Chem. Soc. **130**, 74 (2008).

[20] R. Sens and K. H. Drexhage, J. Lumin. **24-25**, 709 (1981).

[21] A. Lobo, H. Borchert, D. V. Talapin, H. Weller, and T. Moller, Colloids Surf., A **286**, 1 (2006).

[22] H. Borchert, D. V. Talapin, N. Gaponik, C. McGinley, S. Adam, A. Lobo, T. Moller, and H. Weller, J. Phys. Chem. B **107**, 9662 (2003).

[23] R. H. Bube, *Photoconductivity of Solids* (Wiley, New York, 1960).

[24] W. Martienssen, in *Landolt-Börnstein: Numerical Data and Functional Relationships in Science and Technology–New Series* (Springer-Verlag, Berlin, 1961).

[25] M. J. Powell, Phys. Rev. B **20**, 4194 (1979).

[26] C. R. Kagan, C. B. Murray, M. Nirmal, and M. G. Bawendi, Phys. Rev. Lett. **76**, 1517 (1996).

[27] T. A. Klar, T. Franzl, A. L. Rogach, and J. Feldmann, Adv. Mater. **17**, 769 (2005).

[28] T. S. Mentzel, V. J. Porter, S. Geyer, K. MacLean, M. G. Bawendi, and M. A. Kastner, Phys. Rev. B **77**, 075316 (2008).